Int. J. Electrochem. Sci., 10 **(2015)** 4696 - 4705

International Journal of
ELECTROCHEMICAL
SCIENCE
www.electrochemsci.org

Preparation and Electrochemical Performances of $LiNi_{0.5}Mn_{0.5}O_2$ Cathode Materials for Lithium-Ion Batteries

Lei Shi[1], *Wenting Xie*[1], *Qisheng Ge*[1], *Sen Wang*[1], *Da Chen*[1, *], *Laishun Qin*[1], *Meiqiang Fan*[1], *Liqun Bai*[2, *], *Zhi Chen*[1], *Hangyan Shen*[1], *Guanglei Tian*[1], *Chunju Lv*[1], *Kangying Shu*[1]

[1] School of Materials Science and Engineering, China Jiliang University, Hangzhou, Zhejiang province 310018, China
[2] Key Laboratory of Chemical Utilization of Forestry Biomass of Zhejiang Province, Zhejiang A & F University, Lin'an, Zhejiang Province, 311300, China
[*]E-mail: dchen_80@hotmail.com, bailiqun78@163.com

Received: 27 January 2015 / *Accepted:* 24 March 2015 / *Published:* 28 April 2015

In this work, $LiNi_{0.5}Mn_{0.5}O_2$ were successfully prepared were successfully prepared by an improved solid-state reaction technique using the solid solution of nickel manganese oxide ($Ni_{1.5}Mn_{1.5}O_4$) as the precursor. The phase structure and surface morphologies of as-prepared $LiNi_{0.5}Mn_{0.5}O_2$ were identified by X-ray diffraction (XRD) and field-emission scanning electron microscope (FESEM) measurements. The as-prepared $LiNi_{0.5}Mn_{0.5}O_2$ presented an α-$NaFeO_2$-type ($R\bar{3}m$) layered crystalline structure, and possessed an irregular granular appearance with a narrow size distribution and an average grain size of ca. 1.2 μm. The as-prepared $LiNi_{0.5}Mn_{0.5}O_2$ cathode material delivered an initial discharge capacity of 182.4 mAh g^{-1} at 0.2 C, and retained a discharge capacity of 175.4 mAh g^{-1} (about 96.2% of the intial discharge capacity) after 100 cycles. At a high rate of 4 C, a specific discharge capacity of 115 mAh g^{-1} (about 63% of the initial capacity at the rate of 0.2 C) was also retained. The electrochemical measurements demonstrated that the as-prepared $LiNi_{0.5}Mn_{0.5}O_2$ cathode material offered highly reversible capacities, good cycling stabilities, and excellent rate capabilities. The smashing electrochemical performance could be attributed to the as-prepared solid solution of precursor $Ni_{1.5}Mn_{1.5}O_4$, which resulted in a uniform distribution of nickel and manganese elements onto the ideal layer structure of as-prepared $LiNi_{0.5}Mn_{0.5}O_2$.

Keywords: $Ni_{1.5}Mn_{1.5}O_4$, Lithium nickel manganese oxide, Solid state reaction, Cathode materials, Lithium ion batteries

1. INTRODUCTION

Recently, rechargeable lithium ion batteries (LIBs) have been widely developed as popular power sources for portable electronic devices such as cell phones, laptop computers, and are also regarded as promising energy storage devices for electronic vehicles (EV) and hybrid electronic

vehicles (HEV) due to their high energy density, power capability, superior safety and stable cycling lifespan [1-3]. Currently, the common cathode material in commercial LIBs is $LiCoO_2$ owing to its high Li^+ mobility, high electrochemical potential versus Li/Li^+ (~ 4 V), and a relatively high capacity of above 140 mAh g^{-1} with a good reversibility [4]. However, cobalt compounds are thermally unstable, toxic, less available and costly [5]. These inherent disadvantages have greatly suppressed the widespread application of $LiCoO_2$ in lithium secondary batteries. Hence, it is extremely necessary to develop alternative cathode materials for LIBs with better electrochemical performances and environmental safety.

In recent years, extensive attention has been paid to the layered lithium nickel manganese oxide ($LiNi_xMn_{1-x}O_2$) compounds due to their attractive characteristics, such as low cost, high discharge capacity, long cycling stability and thermal safety [6, 7]. Among these layered $LiNi_xMn_{1-x}O_2$ compounds, $LiNi_{0.5}Mn_{0.5}O_2$, which was first proposed by Ohzuku and Makimura [8], has been regarded as one of the most attractive alternative cathode materials for lithium-ion batteries [9-11] because it has high capacity and a stable structure [9]. In this material, Ni^{2+} is the only active element to contribute to the capacity, and Mn^{4+} is an electrochemically inactive element that acts as the stable octahedral ions to ensure the stability of the lattice structure during charge/discharge cycle [12, 13]. Although $LiNi_{0.5}Mn_{0.5}O_2$ exhibits several merits in its electrochemical performance, it is still a challenge to prepare electrochemically active $LiNi_{0.5}Mn_{0.5}O_2$ with desired stoichiometry and high performance. Thus, selection of appropriate preparation method and conditions are critical for attaining an ideal layered crystalline structure of $LiNi_{0.5}Mn_{0.5}O_2$ with good electrochemical performance.

Nowadays, various methods have been used to synthesize $LiNi_{0.5}Mn_{0.5}O_2$, such as solid phase reaction [8, 10, 14], ion exchange method [15], hydrothermal method [16], ultrasonic method [17], and so on. However, control over the layered structure of $LiNi_{0.5}Mn_{0.5}O_2$-based cathodes still remains a challenge. It has been reported that the solid solution of Ni, Mn hydroxides or citrates is of the single phase, in which the distribution of Ni/Mn is homogeneous at atomic level, whereas the mixed hydroxides or citrates are composed of particles with different phase [8, 11]. In this case, electrochemical performance of $LiNi_{0.5}Mn_{0.5}O_2$ prepared from the solid solution of Ni, Mn hydroxides or citrates is better than that prepared from the mixed hydroxides or citrates [8, 11, 18]. Herein, in this work, the layered $LiNi_{0.5}Mn_{0.5}O_2$ material was prepared by an improved solid-state reaction technique using the solid solution of nickel manganese oxide ($Ni_{1.5}Mn_{1.5}O_4$) as the precursor. By means of this technique, it is expected to prepare $LiNi_{0.5}Mn_{0.5}O_2$ cathode material with uniform distribution of Ni and Mn at atomic level. The morphology, structure and electrochemical performance of as-prepared $LiNi_{0.5}Mn_{0.5}O_2$ were investigated.

2. EXPERIMENTAL

2.1 Synthesis of the precursor ($Ni_{1.5}Mn_{1.5}O_4$)

Typically, a stoichiometric mixture of manganese acetate ($Mn(CH_3COO)_2{\cdot}4H_2O$) and nickel acetate ($Ni(CH_3COO)_2{\cdot}4H_2O$) were completely dissolved in water. The solvent in the above mixture solution was then removed by means of a rotary evaporator at 75 ^oC, and the light green acetate salt precipitate was obtained. The resulting precipitate was subsequently ground and calcined at 800 ^oC for

12 h in air. After the calcined precipitate was cooled to room temperature naturally, the $Ni_{1.5}Mn_{1.5}O_4$ precursor was formed.

2.2 Synthesis of $LiNi_{0.5}Mn_{0.5}O_2$ cathode materials

The above-obtained precursor ($Ni_{1.5}Mn_{1.5}O_4$) was mixed well with $LiOH{\cdot}H_2O$ in a stoichiometric proportion (1:1.05). The mixture was then ground and pressed into a pellet. The pellet was then thermally pretreated at 480 ^oC for 3 h with a heating rate of 5 ^oC/ min. When it was cooled to ambient temperature, the pellet was fully ground into powders. These powders were pressed into a pellet once again, and the pellet was finally annealed at 850 ^oC for 12 h with a heating rate of 5 ^oC/ min. After the annealing process, the final product of $LiNi_{0.5}Mn_{0.5}O_2$ was thus obtained.

2.3 Characterizations

The crystal phase identification of samples was performed on a X-ray diffraction (XRD) (Bruker Axs D2 PHASER, Germany) with Cu Kα radiation (λ = 0.15406 nm) in the 2θ range from 10° to 80° with a step scan of 0.02°. The morphologies of the samples were characterized by using the field-emission scanning electron microscope (FESEM, JEOL JSM-6700F, Japan) with an operating voltage of 15 kV. Thermogravimetric analysis (TGA) and differential thermal analysis (DTA) were carried out using a thermogravimetric analyzer (Mettler, SMP/PF7548/MET/600W, Switzerland) with a heating rate of 10 °C/min in air.

2.4 Electrochemical measurements

Electrochemical properties of the products were measured using 2032 coin-type half-cells. The working electrodes were prepared by casting the slurry consisting of 70 wt% of active material ($LiNi_{0.5}Mn_{0.5}O_2$), 20 wt% of conductive Super P carbon black as conductive additive, and 10 wt % of poly (vinylidene fluoride) (PVDF) (Alfa Aesar) as binding agent onto an aluminum foil. The electrolyte consisted of a solution of 1 M $LiPF_6$ in ethylene carbonate (EC)/dimethyl carbonate (DMC) (1:1 v/v). Lithium foil was used as counter electrodes and a polypropylene separator (Celgard) was used to separate the anode and cathode. Finally these cells were assembled in an argon-filled glovebox (Super 1220/750, MIKROUNA). The galvanostatically charge and discharge measurement were performed on a Land battery test system in a voltage window of 2.5-4.3 V (vs. Li/Li^+) at room temperature with different rates.

3. RESULTS AND DISCUSSION

3.1 Synthesis and characterizations of as-prepared $LiNi_{0.5}Mn_{0.5}O_2$

For the successful synthesis of $LiNi_{0.5}Mn_{0.5}O_2$, the prerequisite is the formation of homogeneous $Ni_{1.5}Mn_{1.5}O_4$ precursors. Figure 1 shows the TGA and DTA curves of the mixture of Ni,

Mn citrate, and the mixture of Ni, Mn oxide precursors ($Ni_{1.5}Mn_{1.5}O_4$) and lithium hydroxide ($LiOH{\cdot}H_2O$). As shown in Figure 1A, the mixture of Ni, Mn citrate shows endothermal signals accompanied with weight loss of ca. 28.6% in the regions between 50 and 150 ^oC, which could be ascribed to the removal of superficial and chemisorbed water.

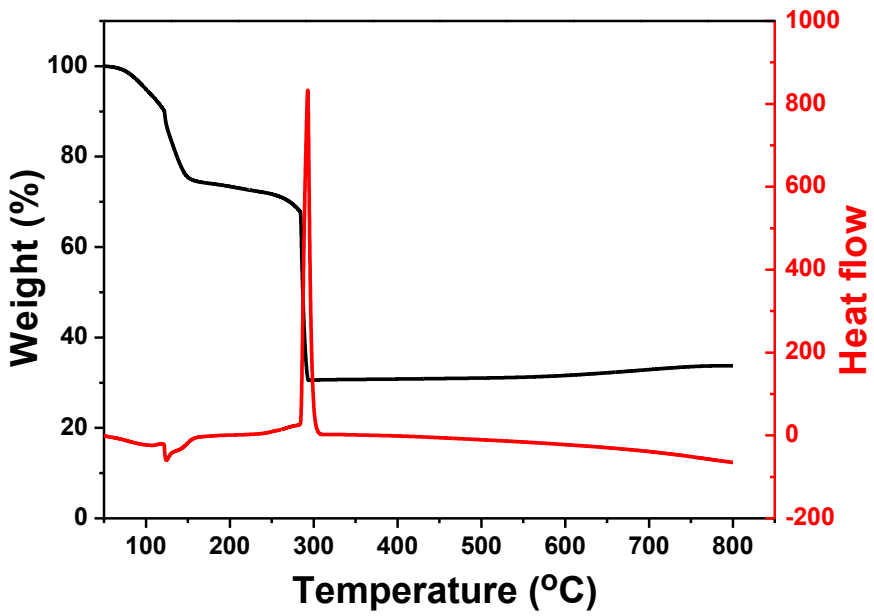

(A)

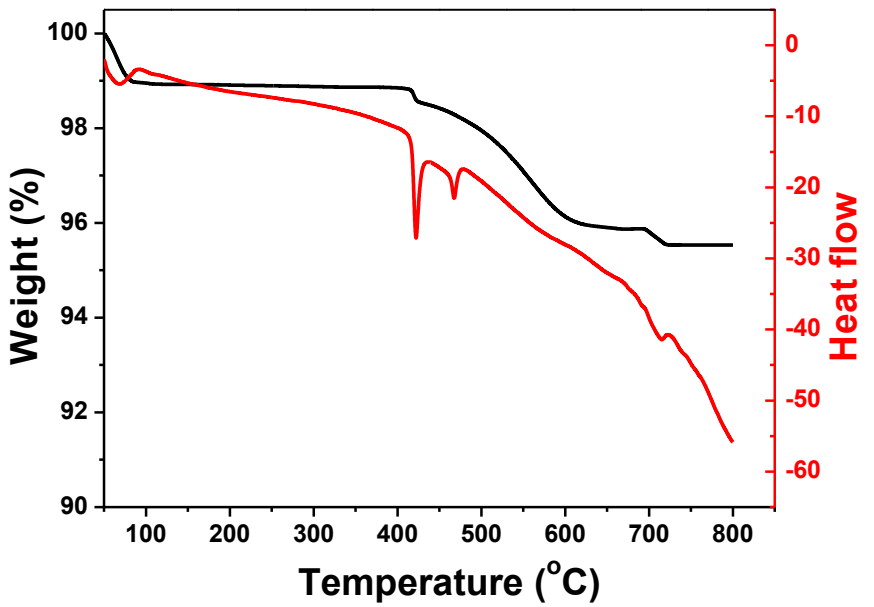

(B)

Figure 1. Thermogravimetric analysis (TGA) and differential thermal analysis (DTA) curves of (A) the mixture of manganese acetate and nickel acetate with the molar ratio of 1:1, and (B) mixture of $Ni_{1.5}Mn_{1.5}O_4$ and lithium hydroxide ($LiOH{\cdot}H_2O$).

Above 180 ^{o}C, the thermal decomposition of the citrate precursor proceeds at two steps. Between 190 and 260 ^{o}C, an endothermic peak accompanied with weight loss of ca. 7.2% appears. According to the literature data on thermal decomposition of citrates [19, 20], this peak could be ascribed to the transformation in the citrate anion leading to a release of citric acid fragments. Between 260 and 320 ^{o}C, an intense exothermal peak accompanied with 37.4% of mass loss is observed. This peak could be attributed to the decomposition of the residual organic compound. At temperatures above 350 ^{o}C, the TGA and DTA curves become flat and no further weight loss can be observed, indicating that the mixture of manganese acetate and nickel acetate could almost be totally decomposed at ~350 ^{o}C to form the precursor of nickel manganese oxide.

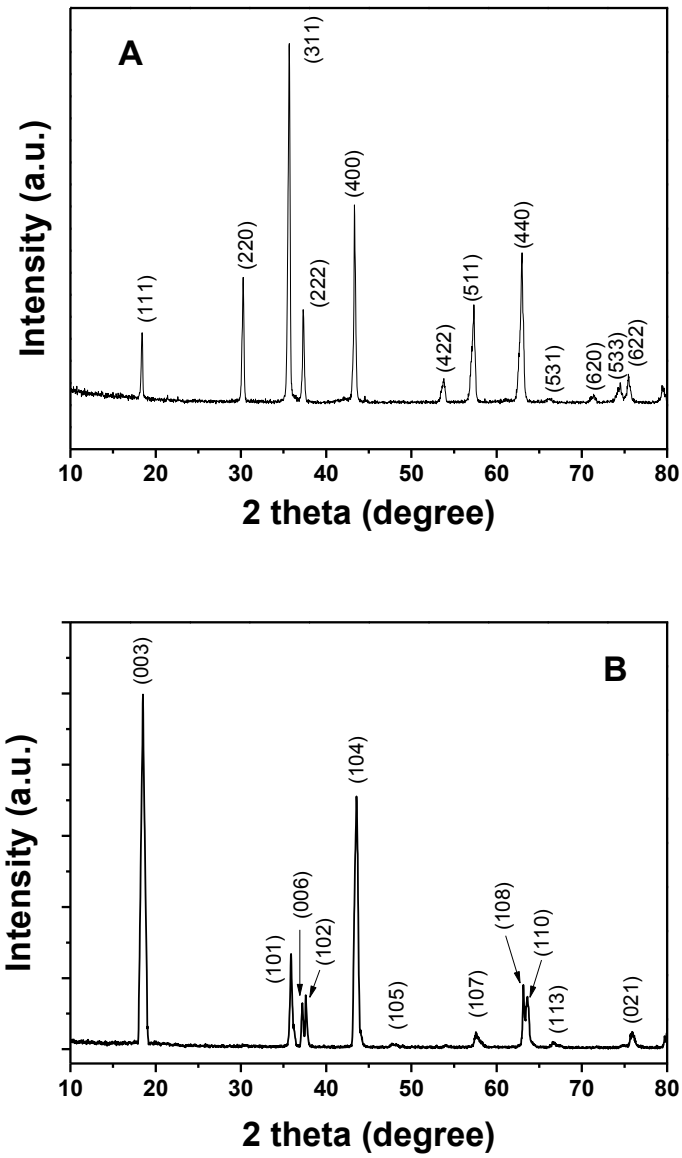

Figure 2. XRD patterns of the precursor $Ni_{1.5}Mn_{1.5}O_4$ (A) and the product $LiNi_{0.5}Mn_{0.5}O_2$ (B).

From the TGA and DTA curves of the mixture of $LiOH{\cdot}H_2O$ and $Ni_{1.5}Mn_{1.5}O_4$ (Figure 1B), it can be seen that there are three weight loss stages during the whole thermal treatment, which could be attributed to the removal of physisorbed and chemisorbed water from lithium hydroxide at 50~150 ^oC, the elimination of water produced from the high-temperature reaction between lithium hydroxide and the $Ni_{1.5}Mn_{1.5}O_4$ precursor at 400~580 ^oC, and the formation of $LiNi_{0.5}Mn_{0.5}O_2$ at higher temperatures of 600~730 ^oC, respectively. When the temperature was up to 730 ^oC, the weight kept unchanged, indicating that the solid-state reaction between lithium hydroxide and the $Ni_{1.5}Mn_{1.5}O_4$ precursor was completely finished [21]. This means that the calcination temperature for the solid-state reaction between lithium hydroxide and the $Ni_{1.5}Mn_{1.5}O_4$ precursor should be up to 730 ^oC in order to produce high crystalline $LiNi_{0.5}Mn_{0.5}O_2$.

The phase structures of the precursor ($Ni_{1.5}Mn_{1.5}O_4$) and the final product ($LiNi_{0.5}Mn_{0.5}O_2$) were identified by XRD measurement. Figure 2A shows the XRD pattern of the $Ni_{1.5}Mn_{1.5}O_4$ precursor. It can be seen that all the diffraction peaks in the pattern could be identified to the spinel structure (JCPDS card No.84-0542) without any impurity phase [11]. The purpose of making $Ni_{1.5}Mn_{1.5}O_4$ is to ensure sufficient mixing of Mn–Ni in the precursor at the atomic level, thus leading to the probable preparation of the pure phase $LiNi_{0.5}Mn_{0.5}O_2$. As shown in Figure 2B, the diffraction peaks appeared in the XRD pattern of the final product ($LiNi_{0.5}Mn_{0.5}O_2$) were well indexed to the α-$NaFeO_2$-type structure (space group $R\bar{3}m$) in good agreement with the literature [22], and no impurity diffraction peaks were detected, indicating that the unwanted Li_2MnO_3 phase does not exist in the final sample under the detection limitation [23]. Meanwhile, the calculated I_{003}/I_{104} intensity ratio (1.43) indicates a high degree of Li–M (Ni, Mn) order in their respective layers [15, 24]. In addition, the splitting of the (006)/(102) and (108)/(110) diffraction pairs can be evidently detected in the XRD pattern of the final product ($LiNi_{0.5}Mn_{0.5}O_2$), indicating the ideal layered structure and crystallinity of $LiNi_{0.5}Mn_{0.5}O_4$ [17].

The morphologies of as-prepared $Ni_{1.5}Mn_{1.5}O_4$ and $LiNi_{0.5}Mn_{0.5}O_2$ were examined by using FESEM, as shown in Figure 3. As seen, the microscopic morphology of the as-prepared precursor ($Ni_{1.5}Mn_{1.5}O_4$) implies an irregular particle structure with a narrow size distribution and an average grain size of ca. 1.2 μm. The final sample ($LiNi_{0.5}Mn_{0.5}O_2$) also presents an irregular morphological structure with a narrow size distribution, similar to the precursor of $Ni_{1.5}Mn_{1.5}O_4$.

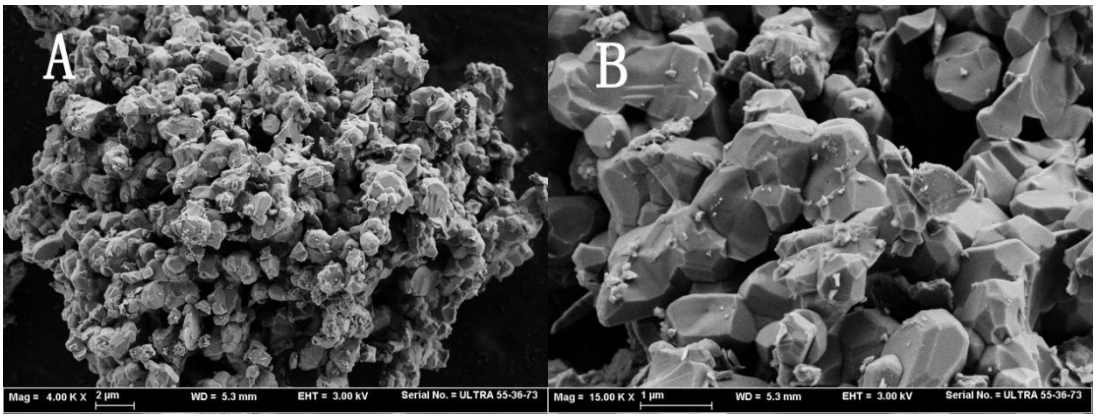

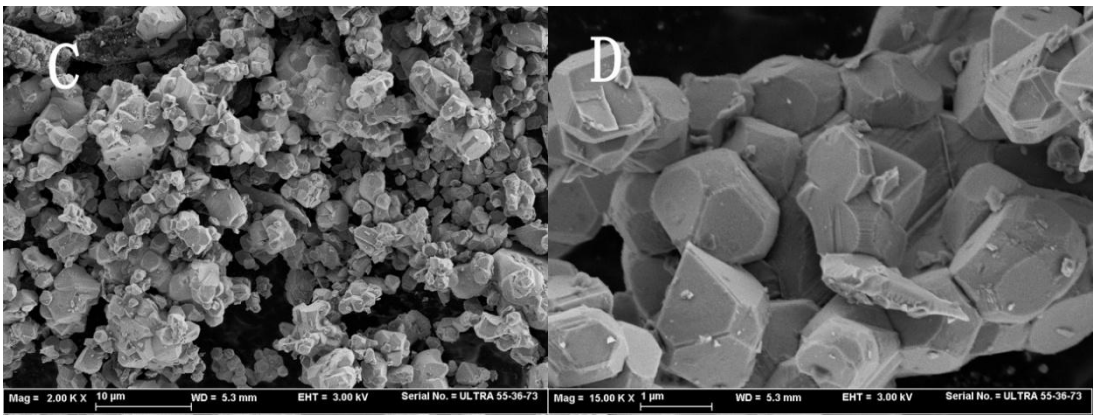

Figure 3. FESEM images of as-prepared $Ni_{1.5}Mn_{1.5}O_4$ at low magnification (A) and high magnification (B), and $LiNi_{0.5}Mn_{0.5}O_2$ at low magnification (C) and high magnification (D).

3.2 Electrochemical measurements

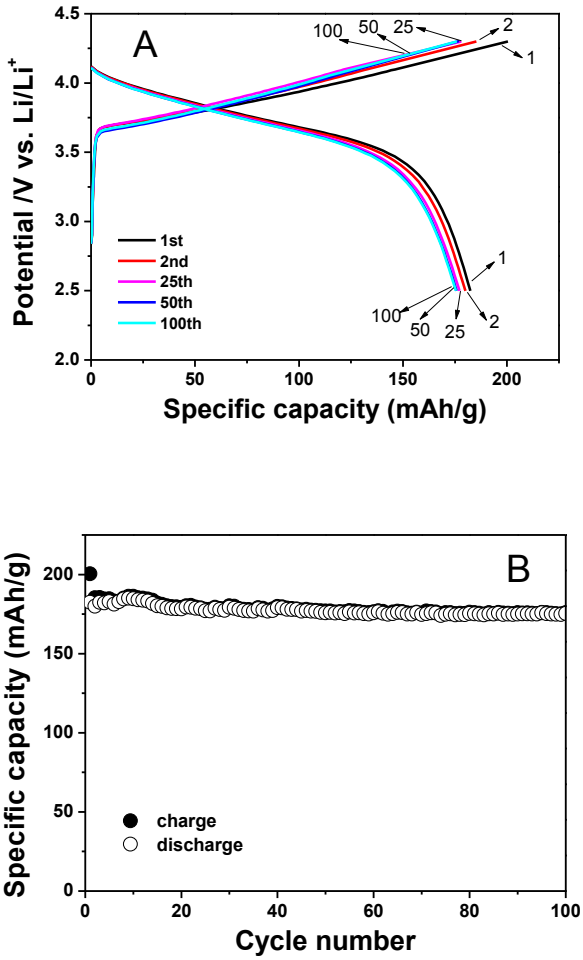

Figure 4. (A) Charge–discharge galvanostatic curves for as-prepared $LiNi_{0.5}Mn_{0.5}O_2$ cycled at room temperature obtained from a 2032 coin-type half cell using Li metal as anode at a rate of 0.2 C in the voltage range of 2.5–4.3 V. (B) Cycling performance of the half cells based on as-prepared $LiNi_{0.5}Mn_{0.5}O_2$ cathodes in the voltage range of 2.5–4.3 V at a rate of 0.2 C.

The electrochemical performance of as-prepared $LiNi_{0.5}Mn_{0.5}O_2$ cathodes were investigated by cycling at room temperature from a coin-type half cell using Li metal as the anode. Representative charge-discharge profiles of the $LiNi_{0.5}Mn_{0.5}O_2$ cathode with 100 cycles at rate of 0.2 C (1C = 180 mA g^{-1}) in the voltage window of 2.5-4.3 V are shown in Figure 4(A). It can be seen that there was a flattening plateau around 3.7 V, representing a typical electrochemical behavior of layered $LiNi_{0.5}Mn_{0.5}O_2$ [14, 18, 25, 26]. The battery based on the as-prepared $LiNi_{0.5}Mn_{0.5}O_2$ cathode material exhibited a discharge capacity of 182.4, 180.7, 177.3, 176.5 and 173.6 mAh g^{-1} when the cycle number was 1, 2, 25, 50 and 100, respectively. The results are better than the performance of the $LiNi_{0.5}Mn_{0.5}O_2$ compound prepared by an improved solid state reaction [6] or a solution combustion procedure [27].

The cycling performance of the battery based on the as-prepared $LiNi_{0.5}Mn_{0.5}O_2$ cathode tested at a rate of 0.2C in the potential range of 2.5-4.3 V is shown in Figure 4(B). The initial charge capacity was 209.5 mAh g^{-1} with a relatively low Coulombic efficiency of 87.1%. The initial irreversible capacity loss could be attributed to the inevitable formation of a solid electrolyte interface (SEI) film at the electrode [28]. Meanwhile, a slight increase in discharge capacity can be observed between the 2nd and subsequent cycles, due to the tendency of stabilization of $LiNi_{0.5}Mn_{0.5}O_2$ after several cycles [26]. Remarkably, it can be seen that the discharge capacity has almost remained unchanged after 20 cycles. After 100 cycles, a discharge capacity of 173.6 mAh g^{-1} was retained, which was about 95.2% of the first discharge capacity. These results indicate an excellent cycling ability of the as-prepared $LiNi_{0.5}Mn_{0.5}O_2$ cathode material, which possesses a high degree of cation ordering required for good Li^+ mobility [11, 25].

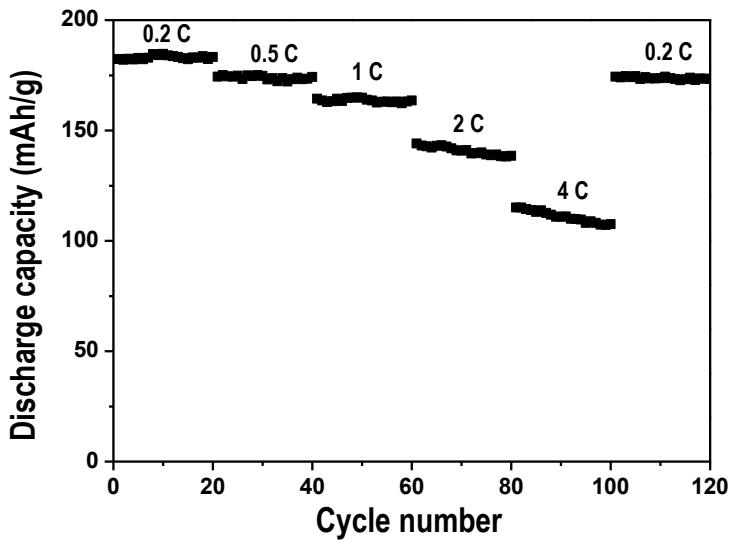

Figure 5. Rate capabilities of the half cells based on as-prepared $LiNi_{0.5}Mn_{0.5}O_2$ at rates ranging from 0.2 C to 4 C in the same voltage window of 2.5–4.3 V.

To further investigate the electrochemical performance of as-prepared $LiNi_{0.5}Mn_{0.5}O_2$ cathode material at higher current rates, the battery based on as-prepared $LiNi_{0.5}Mn_{0.5}O_2$ was cycled at different

rates ranging from 0.2 C (36 mA g^{-1}) to 4 C (720 mA g^{-1}). Discharge capacities as a function of cycle number of the as-prepared $LiNi_{0.5}Mn_{0.5}O_2$ cathode material are shown in Figure 5. The as-prepared $LiNi_{0.5}Mn_{0.5}O_2$ cathode delivers a discharge capacity of about 182.4, 174.4, 164.3, 144.0, and 115.1 mAh g^{-1} at a rate of 0.2 C, 0.5 C, 1 C, 2 C, and 4 C, respectively. At a low current rate (such as: 0.2 C, 0.5 C and 1 C), the discharge capacities barely changed for 20 cycles; while at a high current rate (such as: 2 C and 4 C), the discharge capacities faded slowly for 20 cycles. For example, at a high rate of 4 C, a specific discharge capacity of 107.5 mAh g^{-1} (about 93.4% of the initial capacity at the same rate, and about 58.9% of the initial capacity at a rate of 0.2 C) was retained. The present result in this study is much better than that of SS-Li($Ni_{0.5}Mn_{0.5}$)O_2 prepared by solid-state reaction [14]. It is known that the ratio of I_{003}/I_{104} stands for cation ordering in the layer structure of $LiNi_{0.5}Mn_{0.5}O_2$ [15, 24]. The ratio is about 1.26 for SS-Li($Ni_{0.5}Mn_{0.5}$)O_2 [14], and 1.43 in this study. Apparently, the as-prepared $LiNi_{0.5}Mn_{0.5}O_2$ in this work possesses higher cation ordering in their respective layers. This fact suggests that the better capacity performance at a high current rate could be attributed to improved cation ordering [11]. Remarkably, the as-prepared $LiNi_{0.5}Mn_{0.5}O_2$ cathode also exhibited an excellent capacity restorability. The specific discharge capacity of the cathode was well restored to 174.7 mAh g^{-1} (about 95.8% of the initial capacity at the rate of 0.2 C) when the cathode was cycled from a high current rate of 4 C to a low current rate of 0.2 C. This implies that the as-prepared $LiNi_{0.5}Mn_{0.5}O_2$ possessed good electrochemical reversibility and structure stability. The excellent rate performance suggests that the as-prepared $LiNi_{0.5}Mn_{0.5}O_2$ would be well suitable for cathode materials of high power lithium ion batteries.

4. CONCLUSIONS

In summary, $LiNi_{0.5}Mn_{0.5}O_2$ cathode material with layered α-$NaFeO_2$ type structures were successfully prepared by an improved solid-state reaction technique using the solid solution of nickel manganese oxide ($Ni_{1.5}Mn_{1.5}O_4$) as the precursor. The experimental results revealed that the as-prepared $LiNi_{0.5}Mn_{0.5}O_2$ possessed an α-$NaFeO_2$-type ($R\bar{3}m$) layered crystalline structure, and had irregular granular morphologies with a narrow size distribution and an average grain size of ca. 1.2 μm. The battery based on $LiNi_{0.5}Mn_{0.5}O_2$ delivered an initial discharge capacity of 182.4 mAh g^{-1} at 0.2 C, and maintained a discharge capacity of 175.4 mAh g^{-1} (96.2% of the first discharge capacity) after 100 cycles. A specific discharge capacity of 115 mAh g^{-1} was retained at a rate of 4 C, which was about 63% of the capacity at the rate of 0.2 C. This means that the as-prepared $LiNi_{0.5}Mn_{0.5}O_2$ cathode material possessed highly reversible capacities, good cycling stabilities, and excellent rate capabilities. The smashing electrochemical performance could be attributed to the as-prepared solid solution of the $Ni_{1.5}Mn_{1.5}O_4$ precursor, which resulted in a uniform distribution of nickel and manganese elements onto the ideal layer structure of as-prepared $LiNi_{0.5}Mn_{0.5}O_2$. This work demonstrates that the as-prepared $LiNi_{0.5}Mn_{0.5}O_2$ from a solid solution precursor of nickel manganese oxide offers excellent lithium storage capacity, cyclic stability, and rate capability, indicating its great potential for use as a cathode material for high-performance LIBs.

ACKNOWLEDGEMENTS
This work was financially supported by the International S&T Cooperation Program of China (No. 2013DFG52490), the Excellent Science and Technology Innovation Team of Huzhou, Zhejiang Province (No. 2013KC08) and Pre-research Project of Research Center of Biomass Resource Utilization, Zhejiang A & F University (2013SWZ02-3).

References

1. M. S. Whittingham, *Chem. Rev.*, 104 (2004) 4271-4320.
2. B. Scrosati, *Nature*, 373 (1995) 557-558.
3. M. Armand and J. M. Tarascon, *Nature*, 451 (2008) 652-657.
4. M. Winter, J. O. Besenhard, M. E. Spahr and P. Novák, *Adv. Mater.*, 10 (1998) 725-763.
5. J. Cho, J. G. Lee, B. Kim and B. Park, *Chem. Mater.*, 15 (2003) 3190-3193.
6. Q. Wu, X. L. Li, M. M. Yan and Z. Y. Jiang, *Electrochem. Commun.*, 5 (2003) 878-882.
7. T. F. Song and H. L. Zhang, *Int. J. Electrochem. Sci.*, 8 (2013) 12367-12376.
8. T. Ohzuku and Y. Makimura, *Chem. Lett.*, 30 (2001) 744-745.
9. A. Abdel-Ghany, K. Zaghib, F. Gendron, A. Mauger and C. M. Julien, *Electrochim. Acta*, 52 (2007) 4092-4100.
10. H. Xia, S. B. Tang and L. Lu, *J. Alloys Compd.*, 449 (2008) 296-299.
11. X. L. Meng, S. M. Dou and W. L. Wang, *J. Power Sources*, 184 (2008) 489-493.
12. B. J. Hwang, T. H. Yu, M. Y. Cheng and R. Santhanam, *J. Mater. Chem.*, 19 (2009) 4536-4544.
13. Y. M. Liu, B. L. Chen, F. Cao, X. Z. Zhao and J. K. Yuan, *J. Mater. Chem.*, 21 (2011) 10437-10441.
14. K. Kang, Y. S. Meng, J. Breger, C. P. Grey and G. Ceder, *Science*, 311 (2006) 977-980.
15. Y. Hinuma, Y. S. Meng, K. Kang and G. Ceder, *Chem. Mater.*, 19 (2007) 1790-1800.
16. J. Chou, Y. Kim and G. Kim, *J. Phys. Chem. C.*, 111 (2007) 3192-3196.
17. B. Zhang, G. Chen, P. Xu and Z. Lv, *Solid State Ionics*, 178 (2007) 1230-1234.
18. Y. Makimura and T. Ohzuku, *J. Power Sources*, 119-121 (2003) 156-160.
19. E. Zhecheva, M. Gorova and R. Stoyanova, *J. Mater. Chem.*, 9 (1999) 1559-1567.
20. M. Yoncheva, R. Stoyanova, E. Zhecheva, R. Alcántara and J. L. Tirado, *J Alloys Compd.*, 475 (2009) 96-101.
21. S. Gopukumar, K. Y. Chung and K. B. Kim, *Electrochim. Acta*, 49 (2004) 803-810.
22. Y. Zhou and H. Li, *J. Mater. Chem.*, 12 (2002) 681-686.
23. J. Cho, Y. Kim and G. Kim, *J. Phys. Chem. C*, 111 (2007) 3192-3196.
24. M. Yoshio, Y. Todorov, K. Yamato, H. Noguchi, J. Itoh, M. Okada and T. Mouri, *J. Power Sources*, 74 (1998) 46-53.
25. S. B. Schougaard, J. Bréger, M. Jiang, C. P. Grey and J. B. Goodenough, *Adv. Mater.*, 18 (2006) 905-909.
26. Y. M. Liu, F. Cao, B. L. Chen, X. Z. Zhao, S. L. Suib, H. L. W. Chan and J. K. Yuan, *J. Power Sources*, 206 (2012) 230-235.
27. P. Manikandan, M. V. Ananth, T. P. Kumar, M. Raju, P. Periasamy and K. Manimaran, *J. Power Sources*, 196 (2011) 10148-10155.
28. L. Xiao, X. J. Liu, X. Zhao, H. X. Liang and H. X. Liu, *Solid State Ionics*, 192 (2011) 335-338.

© 2015 The Authors. Published by ESG (www.electrochemsci.org). This article is an open access article distributed under the terms and conditions of the Creative Commons Attribution license (http://creativecommons.org/licenses/by/4.0/).